Advances in Nano Research, *Vol. 3, No. 2 (2015) 97-109*
DOI: http://dx.doi.org/10.12989/anr.2015.3.2.097

Effect of citrate coated silver nanoparticles on biofilm degradation in drinking water PVC pipelines

Supraja Nookala[1], Naga Venkata Krishna Vara Prasad Tollamadugu[*2], Giridhara Krishna Thimmavajjula[2] and David Ernest[1]

[1]*Department of Biotechnology, Thiruvalluvar University, Vellore-632001, India*
[2]*Nanotechnology laboratory, Institute of Frontier Technology, Regional Agricultural Research Station, Acharya N.G. Ranga Agricultural University, Tirupati – 517 502, A.P., India*

(Received June 11, 2015, Revised July 8, 2015, Accepted July 10, 2015)

Abstract. Citrate ion is a commonly used reductant in metal colloid synthesis, undergoes strong surface interaction with silver nanocrystallites. The slow crystal growth observed as a result of the interaction between the silver surface and the citrate ion makes this reduction process unique compared to other chemical and radiolytic synthetic methods. The antimicrobial effects of silver (Ag) ion or salts are well known, but the effects of citrate coated Ag nanoparticles (CAgNPs) are scant. Herein, we have isolated biofilm causative bacteria and fungi from drinking water PVC pipe lines. Stable CAgNPs were prepared and the formation of CAgNPs was confirmed by UV-visible spectroscopic analysis and recorded the localized surface plasmon resonance of CAgNPs at 430 nm. Fourier transform infrared spectroscopic analysis revealed C=O and O-H bending vibrations due to organic capping of silver responsible for the reduction and stabilization of the CAgNPs. X-ray diffraction micrograph indicated the face centered cubic structure of the formed CAgNPs, and morphological studies including size (average size 50 nm) were carried out using transmission electron microscopy. The hydrodynamic diameter (60.7 nm) and zeta potential (-27.6 mV) were measured using the dynamic light scattering technique. The antimicrobial activity of CAgNPs was evaluated (in vitro) against the isolated fungi, Gram-negative and Gram-positive bacteria using disc diffusion method and results revealed that CAgNPs with 170ppm concentration are having significant antimicrobial effects against an array of microbes tested.

Keywords: C-Ag nanoparticles; antimicrobial activity; bacterial sp; fungi sp

1. Introduction

Nanoparticles are emerging materials that have a broad range of applications and notable characteristics different from those of bulk materials. Nanoparticles possess high surface area to volume ratio. Nanoparticles such as silver, gold, cadmium sulfide, zinc sulfide, and zinc oxide play important role in various fields (Malarkodi *et al.* 2014). They often have specific optical and electronic properties (Kelly *et al.* 2003) and chemical reactivity. (Nurmi *et al.* 2004) Silver nanoparticles (Ag-NPs or nanosilver) are one of the most widely used nanoparticles, most notably serving as an antimicrobial agent for medical applications. The toxicity of nanosilver may be

*Corresponding author, Senior Scientist, E-mail: tnvkvprasad@gmail.com

Copyright © 2015 Techno-Press, Ltd.
http://www.techno-press.com/?journal=anr&subpage=7 ISSN: 2287-237X (Print), 2287-2388 (Online)

explained by the interaction of nanoparticles with microbes involving silver ion release and particle cellular internalization (Sondi and Salopek-Sondi 2004, Navarro *et al*. 2008). Size dependent and species specific toxicity of nanosilver (Carlson *et al*. 2008, Choi *et al*. 2008a, Jiang *et al*. 2008) supports the mode of action of Ag-NPs. Relatively small Ag-NPs can inhibit nitrifying bacterial growth more than silver ions at the same total silver concentrations. However, Ag-NPs are not as effective as Ag ions in killing *Escherichia coli*. (Choi *et al*. 2008b) Over the past decade; there has been a strong push towards the development of silver-containing materials for commercial use that exhibit antimicrobial or bactericidal properties. Research has been intensive in antibacterial material containing various natural and inorganic substances (Kim *et al*. 1998). Among them, silver or silver ions have long been known to have strong inhibitory and bactericidal effects as well as a broad spectrum of antimicrobial activities (Uchida 1995, Grier 1983). Several proposals have been developed to explain the inhibitor effects of silver ion/silver metal on bacteria (Venkateswara and Samson Nesaraj 2014). It is generally believed that heavy metals react with proteins by combining the thiol (SH) groups, which leads to the inactivation of the proteins (Lehninger *et al*. 1993). Recent, microbiological and chemical experiments implied that interaction of silver ion with thiol groups played an essential role in bacterial inactivation (Liau *et al*. 1997). Also, it is revealed that bulk silver in an oxygen-charged aqueous media catalyzes the complete destructive oxidation of microorganisms (Davis and Liu1997). Metal nanoparticles (Me-NPs), which have a high specific surface area and a high fraction of surface atoms have been studied extensively because of their unique physicochemical characteristics including catalytic activity, optical properties, electronic properties, antimicrobial activity, and magnetic properties (Kowshik *et al*. 2003, Souza 2004, Duran *et al*. 2005). Among Me-NPs, silver nanoparticles (Ag- NPs) have been known to have inhibitory and bactericidal effects. It can be expected that the high specific surface area and high fraction of surface atoms of Ag-NPs will lead to high antimicrobial activity as compared with bulk silver metal (Cho *et al*. 2005, Ujjal Kumar Sur 2014). The combined effects of Ag-NPs with the antibacterial activity of antibiotics have not been studied. The ability of pathogenic bacteria to resist antimicrobial agents has emerged in recent years and is a major health problem (Wright 2000, Wright 2005).

In this paper, we present a simple and rapid synthesis of Citrate coated silver nanoparticles. As prepared, C-Ag nanoparticles (CAgNPs) were characterized using the techniques, such as UV-Vis spectroscopy, FT-IR, Dynamic light scattering, TEM and XRD. Further, the antimicrobial properties of CAgNPs were studied against an array of microbes which are isolated from the drinking water PVC pipelines.

2. Materials and measurements methods

Silver nitrate (>99% pure) and Trisodium citrate dihydrate (99.0% pure) was purchased from Sigma Aldrich, India. Potato dextrose broths, Potato dextrose agar, Nutrient broth, Nutrient agar plate, were supplied by Hi-media, India.

2.1 Collection of biofilm formed in poly vinyl chloride (PVC) pipes

The PVC biofilm samples were collected from four different regions located in and around Tirupati (Chittoor District), Andhra Pradesh, India. The samples were collected from drinking water supply PVC pipelines and stored in plastic bottles. The collected samples were in amorphous

form. These samples were stored in an ice box and transported for further microbiological characterization analysis.

2.2 Isolation of Fungal and Bacterial sp. from drinking water pipeline biofilm

Nearly eight fungal species and ten bacterial samples were collected from the four different pipelines in Tirupathi, Chittoor district, A.P, India. Through serial dilution pour plate technique, Fungal sp. was isolated using Potato Dextrose Agar Medium (PDA) and Gram negative, Positive bacteria was isolated from Nutrient Agar medium. Further it is maintained in Potato Dextrose Agar slants (Fungi) and Nutrient agar slants (Bacteria).

2.3 Synthesis of Citrate coated silver-nanoparticles (CAg-NPs)

The silver colloid was prepared by using chemical reduction method reported (Yakutik *et al.* 2004). Silver nitrate (>99%) and trisodium citrate dihydrate (99.0%) were purchased from Sigma Aldrich. Sodium citrate and silver nitrate (5:1) were mixed in a conical flask and aged for about 2 hrs. The solution was heated to the elevated temperatures on slow heating. During the heating process, 2-3 drops of 0.01 M sodium borohydrate was added solution gradually turned yellow within a few minutes, indicating the formation of Ag nanoparticles. The solution was kept boiling for an additional 6 minutes. After that, the heating mantle was removed and the solution was allowed to cool. At this point this solution of Ag nanoparticles was so stable that it did not change color for as long as several months without any stabilizing agent. The initial concentration of the CAg nanoparticles was measured using inductively coupled plasma optical emission spectrophotometer (ICP-OES) and was found to be 170$\pm$1.4 ppm. Then, by diluting this solution, each sample of different concentration was used to investigate the concentration dependence of the antibacterial effect of Ag nanoparticles. These CAg nanoparticles were characterized by using the techniques such as *X*-ray diffractometry (XRD), Fourier transform infrared spectrophotometry (FTIR), UV-Vis spectrophotometry, dynamic light scattering (Particle size), zeta potential and transition electron microscopy (TEM).

2.4 Measurement of concentration of CAgNPs using inductively coupled plasma optical emission spectrophotometer (ICP-OES)

The concentrations of the CAgNPs were measured using ICP-OES (Prodigy XP, Leeman Labs, USA). The samples were prepared with 10 times dilution after centrifugation at 4,000 rpm for 15 min. Then, 20 ml of aliquot was loaded to the racks of automatic sampler and estimated the concentration of CAgNPs thrice.

2.5 Assay for antimicrobial activity of C-Ag nanoparticles against microorganisms (Bacteria and Fungi)

The antimicrobial activity of CAg nanoparticles was examined on the basis of colony formation by in vitro Petri dish assays (disc diffusion). Each fungal and bacterial isolates was cultured on growth media that induced prolific conidia and bacterial production. The fungus isolates were grown on potato dextrose agar medium, and bacterial isolates were grown on nutrient agar medium. Conidia were collected from cultures that were incubated at 37℃ for 10 days (fungi),

and bacterial cultures were collected from cultures that were incubated at 37℃ for 2 days for (bacteria) and diluted with sterile, deionized water to a concentration of 106 spores ml-1. Aliquots of the conidial suspension and bacterial suspension were mixed with serial concentrations of silver preparations to a final volume of 1 ml and were also mixed with sterile, deionized water as control. A 10μl subsample of the conidia and CAg mixture stock was taken at 30±0.8, 100±1.1 and 170±1.4 ppm after silver treatments and diluted 100-fold with the deionized water. A 10µl aliquot of the diluted spore suspension was spread on PDA (Becton, Dickson and Company, Sparks, MD) medium. Three PDA plates for fungi and three NA plates for bacteria per each combination of exposure CAg concentration were tested. The filter paper disc dipped in different ppm and inserted on mediums (PDA), and then, the plates were incubated at 37℃ for 2-4 days for fungi and bacteria, respectively. The average number of colonies from silver-treated spore suspensions (fungi) and (bacteria) was compared with the number on the water control (percent colony formation). The zone size was determined by measuring the diameter of the zone in mm (Cynthia and Callaghan 1983, Yamac and Bilgili 2006, Reeves and Andrew1999).

2.6 Characterization of silver nanoparticles

2.6.1 UV-visible spectrum for synthesized nanoparticles

The reduction of silver ions and formation of nanoparticles were monitored by UV-Vis spectrophotometer (UV-2450, SHIMADZU) at various time intervals run from 200 to 800 nm.

2.6.2 FTIR analysis for synthesized nanoparticles

The FTIR spectrum was taken in the mid-IR region of 400-4,000 cm^{-1}. The spectrum was recorded using ATR (attenuated total reflectance) technique. The dried sample was mixed with the KBr (1:200) crystal, and the spectrum was recorded in the transmittance mode.

2.6.3 Particle size and zeta potential analyzer for synthesized nanoparticles

The aqueous suspension of the synthesized nanoparticles was filtered through a 0.22-μm syringe-driven filter unit, and the size (hydrodynamic diameter) and distribution of the nanoparticles were measured using dynamic light scattering technique (Nanopartica, HORIBA, SZ-100).

2.6.4 X-ray diffraction (XRD) analysis for synthesized nanoparticles

The XRD pattern was recorded using computer controlled XRD system (JEOL; Model: JPX-8030 with CuKα radiation (Ni filtered=13418A°) in the range of 40 kV, 20A. The built-in software (syn. master 7935) program was used for the identification of XRD peaks corresponds to the Bragg's reflections.

2.6.5 Transmission electron microscopy (TEM)

The surface morphology and size of the nanoparticles were studied by transmission electron microscopy (JEOL (JEM- 1010)) with an accelerating voltage of 80 kV. A drop of aqueous AgNPs on the carbon-coated copper TEM grids was dried and kept under vacuum in desiccators before loading them onto a specimen holder. The particle size and surface morphology of nanoparticles were evaluated using ImageJ 1.45s software.

Fig. 1 Shows that $AgNO_3$ color changes from colorless to dark brown color (Synthesis of silver nanoparticles by Sodium citrate)

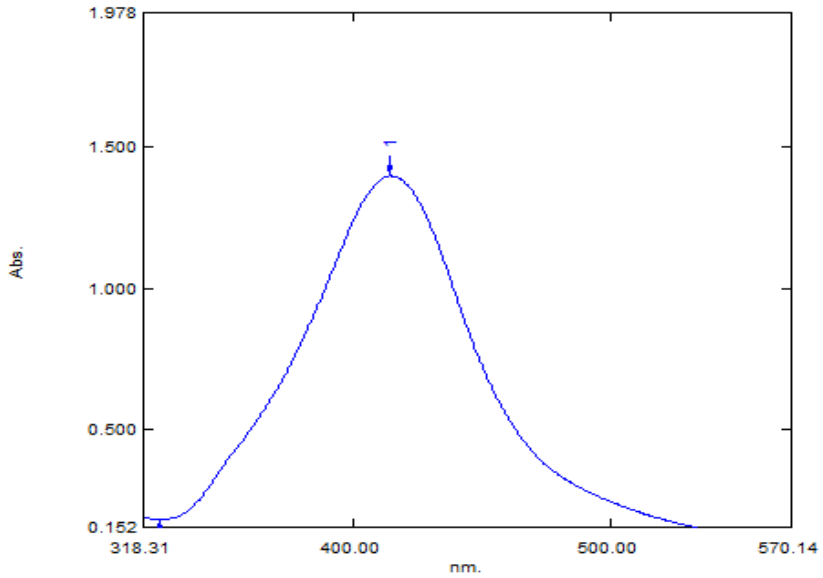

Fig. 2 Showing UV-visible spectroscopy recorded using Citrate coated silver nanoparticles

3. Results and discussion

3.1 Genesis of citrate coated silver nanoparticles

Drinking water pipeline fungi and bacteria species have unusual biological activities depending upon the metabolisms under temperature, pH and pressure. It is well- known that silver nanoparticles exhibit brown color, arising due to excitation of surface Plasmon vibrations in the silver nanoparticles Fig. 1. The sodium citrate, which serves the dual role of a reductant and

stabilizer; stable silver nanoparticles were formed when an aqueous solution of $AgNO_3$ (1mM) is boiled in the presence of sodium citrate. The silver particles prepared by the citrate reduction method produce relatively large-sized (50-100-nm). Because of the wide dispersity of the particle size and shape, we observe broad surface Plasmon absorption with a maximum around 420 nm. The absorption band and particle size of silver nanoparticles prepared using chemical reductants points out the unusual role of citrate ions in controlling the crystal growth and morphology of silver particles. The color variation indicates that silver ions reduction on the medium depend upon the biological activities under temperature conditions.

3.2 UV-Visible spectral analysis

UV-Visible spectroscopy was employed to understand the biosynthesis of Citrate coated silver nanoparticles Fig. 2 shows the UV-Visible adsorption spectra of silver nanoparticles after 24 hrs incubation at room temperatures (37℃). The spectrum shows peak at 430 nm with maximum absorbance. The strong narrow peak represents the monodispersity of the CAgNPs with isotropic in shape. These observations show that sodium citrate brings about slow growth of silver particles and the reaction time is influenced by the concentration of sodium citrate. The overall observations suggest that the bio reduction of (silver ions) Ag^{+} to $Ag^{(0)}$ was confirmed by UV-Visible spectroscopy.

3.3 FT-IR analysis and identification of the functional groups

FT-IR spectrum is used to identify the possible chemical interactions among the silver salts and functional groups present. FT-IR spectrum of the Citrate coated silver nanoparticles using Fig. 3 shows the absorption peaks at 565, 580,1633, 2066, 2308, 3380 cm^{-1}. The peak at 3380 and 2018.5 cm^{-1} due to stretching vibration of OH group and the oxygen stretching and bending frequency.

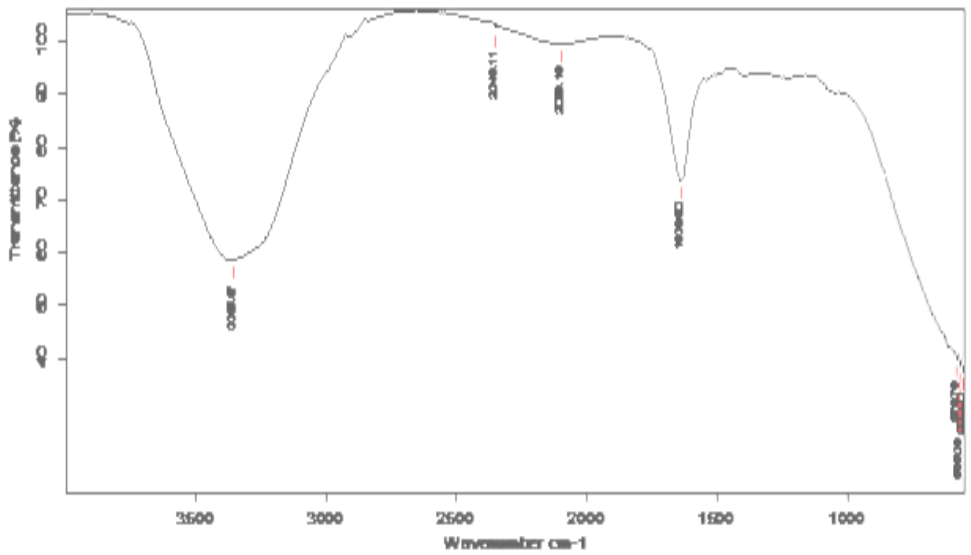

Fig. 3 FTIR spectroscopy recorded using Citrate coated silver nanoparticles

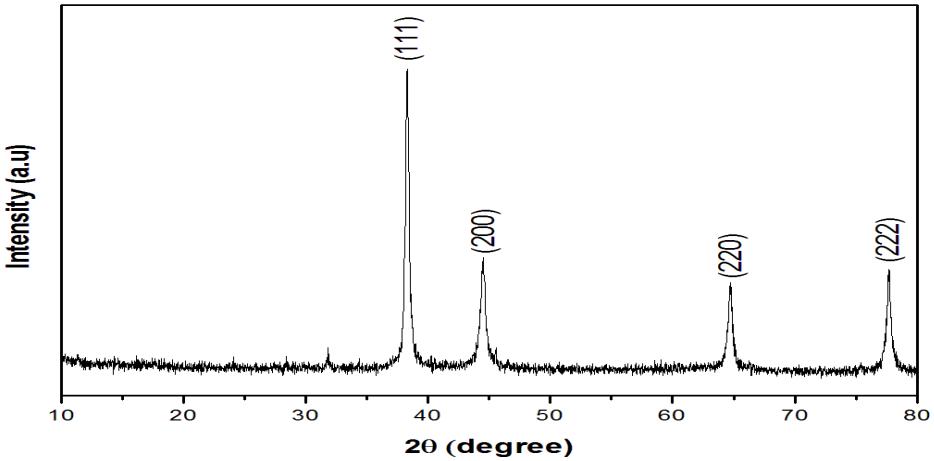

Fig. 4 XRD pattern of capped silver nanoparticles synthesized using Sodium citrate

The band present at 2066 shows -C=C- stretching vibration of alkynes. The band present at 2308 indicates the presence of O-C-O symmetrical stretching vibration of carboxylate respectively. The band present at 565 and 580 shows the C-Br stretching likewise, the bands at 1633 cm^{-1} shows C=O and O-H bending vibrations due to organic capping of silver. The nanoparticles are bound to the functional organic groups (carboxyl and amine) which may acts as template for reducing and capping of nanocrystals.

3.4 X-ray diffraction analysis

XRD pattern of CAgNPs shows the peaks four peaks at 40°, 43°, 64° and 76° were assigned to diffraction signals of (111), (200), (220), and (222) plane for face centered cubic (FCC) silver Fig. 4. The lattice constant calculated from this pattern was 4.0869A°, a value in agreement with literature report (4.0855A°) JSPCDS file no 89-3722. This clearly indicates that the silver nanoparticles formed by the reduction of Ag+ ions are crystalline in nature. The crystal phase analysis of face centered cubic (FCC) and then high intensity of 111 plane structure supports the enhanced antimicrobial activity of CAgNPs. The crystalline size was calculated from the width of the peaks present in the XRD pattern using the Debye–Scherrer formula $D=0.94\lambda/\beta\cos\theta$ where D is the average crystalline domain size perpendicular to the reflecting planes, λ (1.5406×10^{-10}) is the *X*-ray wavelength used, *b* is the full width at half maximum (FWHM) and h is the diffraction angle (Prasad *et al*. 2011).

3.5 Dynamic Light scattering (DLS) analysis

Dynamic Light Scattering analysis measured hydrodynamic diameter of the $AgNO_3$ was found to be 60.9 nm Fig. 5(a). The recorded value of Zeta potential of the silver nanoparticles was -27.6 mV with a single peak Fig. 5(b) signifies the presence of repulsive electro-static forces among the CAgNPs, which leads to the monodispersity of the particles. If the hydrosol has a large negative or positive zeta potential (>25 mV) then they will tend to repel with each other and there will be no tendency of the particles to agglomerate.

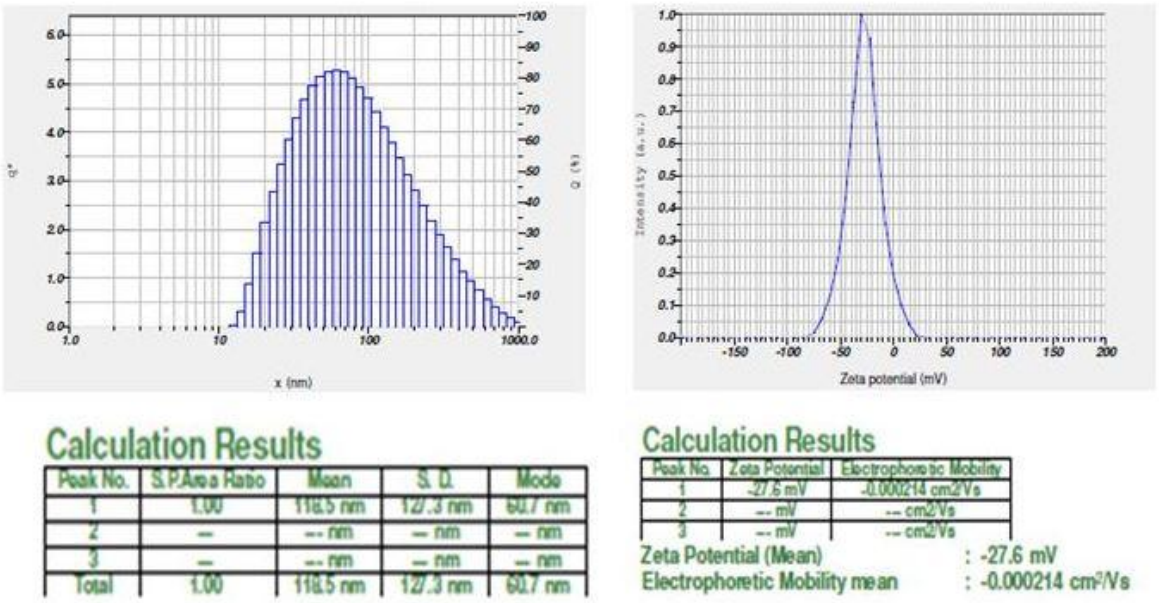

Fig. 5 Showing Dynamic light scattering results showing that particle size and zeta potential of Citrate coated Silver nanoparticles

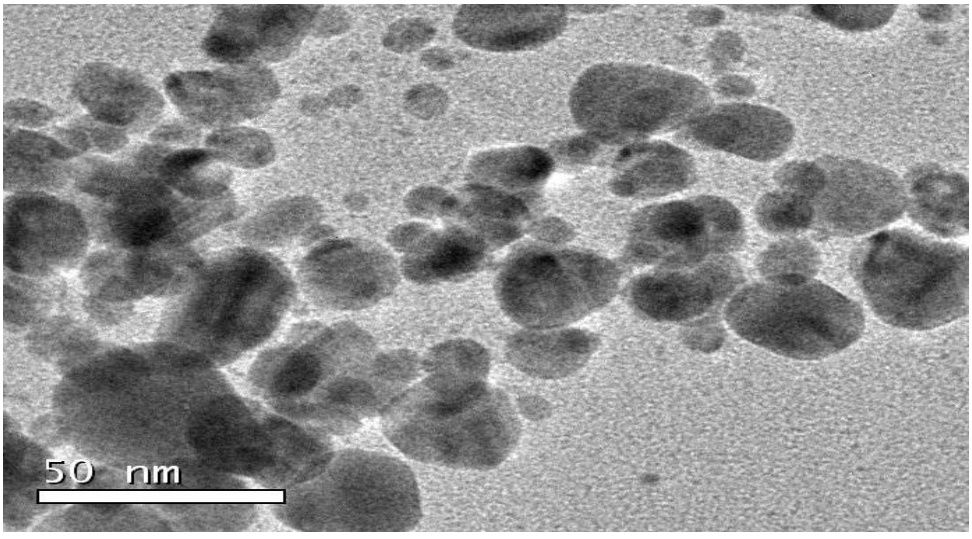

Fig. 6 TEM image of Citrate coated silver nanoparticles showing spherical shaped particles

3.6 Surface morphological studies using TEM

The size and shape of CAgNPs were characterized and shown in the TEM micrograph Fig. 6. It is clearly representing monodispersed individual silver nanoparticles with the occasional aggregates. The shape of the particles was roughly spherical with the measured average particle size of 50 nm.

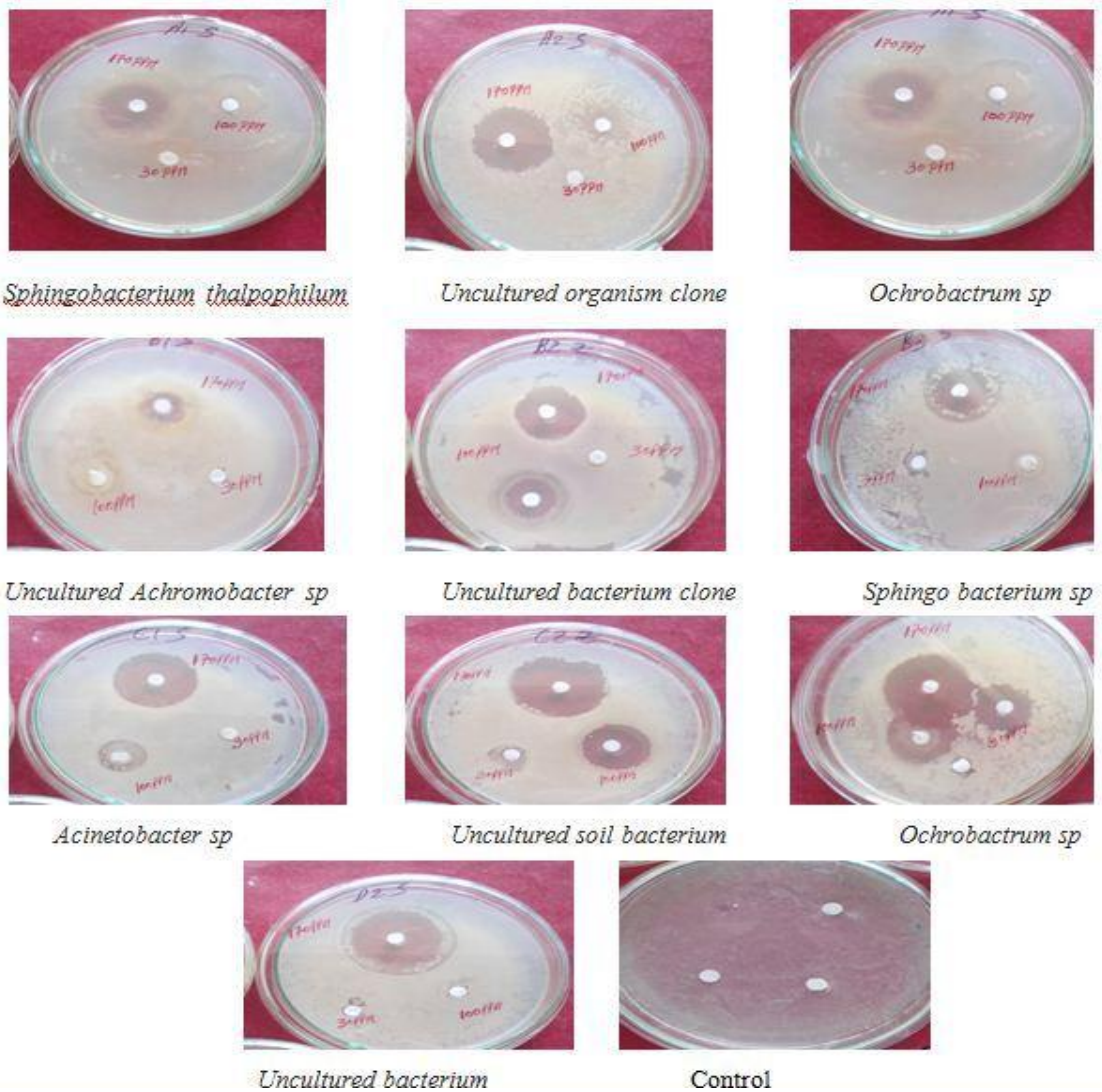

Fig. 7 Synthesized Citrate coated Ag nanoparticles showing effective Antibacterial activity towards Gram positive and Gram negative bacteria

3.7 Antimicrobial efficacy of Citrate coated silver nanoparticles

Citrate coated silver nanoparticles have very strong inhibitory action against fungal sp, Gram-positive and Gram-negative bacteria (Plates 1 and 2). These isolates were collected from drinking water PVC pipes. Three concentrations of CAgNPs (170±1.4 ppm, 100±1.1 ppm, 30±0.8 ppm) were prepared and were applied against an array of fungal species *viz.*, *Meyerozyma caribbica, Aspergillus parvisclerotigenus, Meyerozyma guilliermondii, Rhizopus oryzae, Uncultured fungus clone, Aspergillus oryzae, Trichoderma asperellum* and *Meyerozyma caribbica and bacterial species viz., Sphingobacterium thalpophilum, Uncultured organism clone, Ochrobactrum sp., Uncultured Achromobacter sp., Uncultured bacterium clone, Sphingo bacterium sp.,*

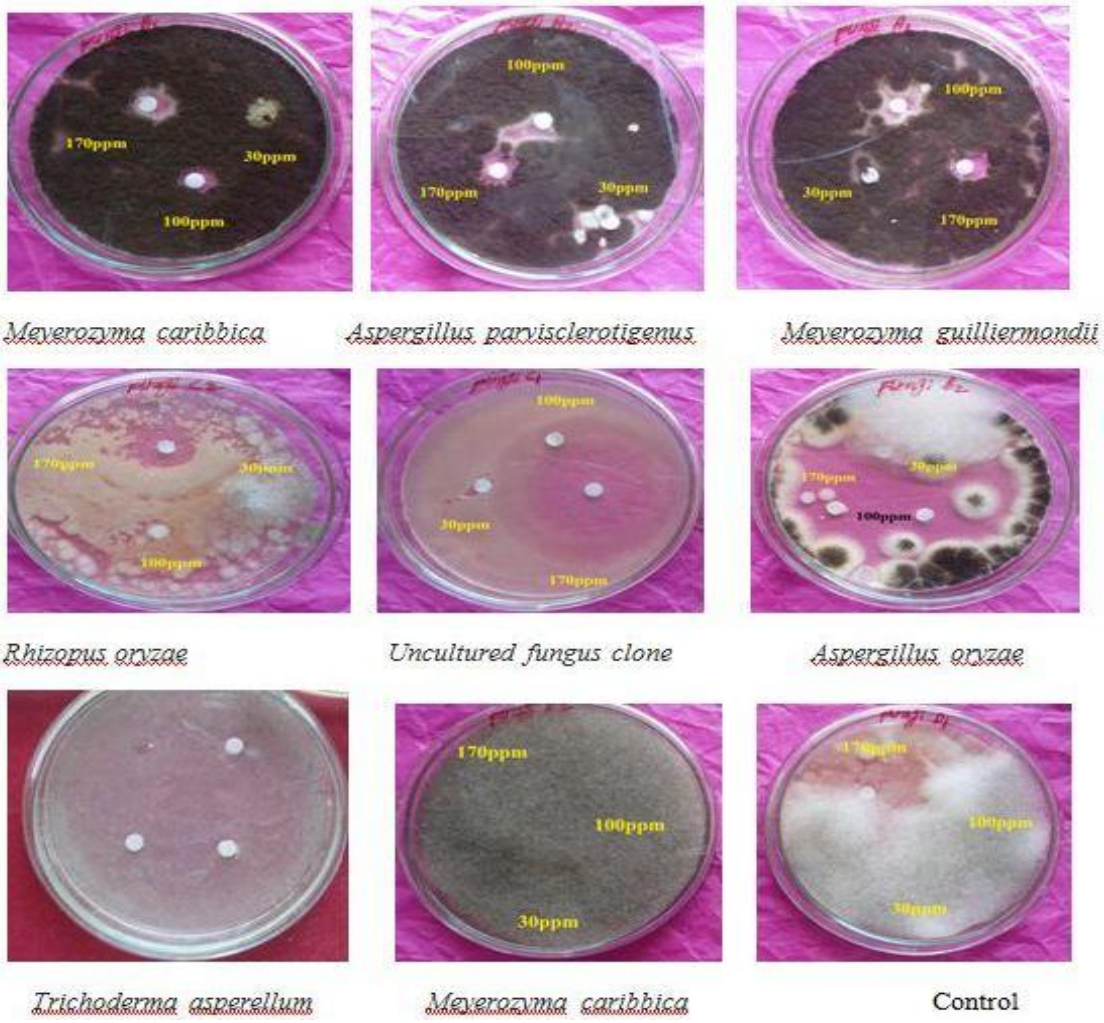

Fig. 8 Citrate coated Ag nanoparticles showing effective Antifungal activity

*Acinetobacter sp.***,** *Uncultured soil bacterium, Ochrobactrum sp.* and *Uncultured bacterium.* The higher concentration (170 ppm) of CAgNPs showed significant antimicrobial effect Tables 1 and 2 compared with other concentrations (100, 30 ppm). The mechanism of inhibitory action of silver ions on microorganisms is partially known. It is believed that DNA loses its replication ability and cellular proteins become inactivated on Ag+ treatment (Feng *et al*. 2000). In addition, it was also shown that Ag+ binds to functional groups of proteins, resulting in protein denaturation (Spadaro *et al*. 1974). There are reports in the literature that show that electrostatic attraction between negatively charged bacterial cells and positively charged nanoparticles is crucial for the activity of nanoparticles as bactericidal materials (Stoimenov *et al*. 2002, Hamouda and Baker 2000). While the mechanism of the interaction between these particles and the constituents of the outer membrane of bacteria and fungi is unfortunately still unresolved, it would appear that, despite their negative surface charge, they somehow interact with "building elements" of the bacterial membrane, causing structural changes and degradation and finally, cell death. Extensive

Table 1 *In-vitro* antibacterial studies of bacteria present in drinking water PVC pipelines using Citrate coated silver nanoparticles as inhibitors

S. no	Bacteria	Citrate coated silver nanoparticles nanoparticles Zone of inhibition (mm)		
		170 ppm	100ppm	30ppm
1.	*Sphingobacterium thalpophilum*	2.0 ± 0.03^{b}	1.0 ± 0.01^{de}	0.6 ± 0.15^{b}
2.	*Uncultured organism clone*	3.0 ± 0.02^{a}	1.8 ± 0.15^{a}	1.0 ± 0.18^{ab}
3.	*Ochrobactrum sp*	0.8 ± 0.06^{c}	0.4 ± 0.06^{g}	0.2 ± 0.01^{c}
4.	*Uncultured Achromobacter sp*	1.6 ± 0.08^{b}	1.2 ± 0.1^{cd}	0.8 ± 0.05^{a}
5.	*Uncultured bacterium clone*	1.0 ± 0.14^{bc}	0.6 ± 0.16^{f}	0.2 ± 0.02^{c}
6.	*Sphingobacterium sp*	2.2 ± 0.16^{b}	0.8 ± 0.18^{ef}	0.4 ± 0.03^{bc}
7.	*Acinetobacter sp*	2.8 ± 0.05^{a}	1.4 ± 0.12^{bd}	0.8 ± 0.06^{a}
8.	*Uncultured soil bacterium*	3.4 ± 0.19^{a}	2.4 ± 0.15^{a}	1.2 ± 0.07^{ab}
9.	*Ochrobactrum sp*	1.2 ± 0.07^{bc}	0.6 ± 0.07^{fg}	0.2 ± 0.09^{c}
10.	*Uncultured bacterium*	4.0 ± 0.03^{a}	1.6 ± 0.11^{ab}	0.6 ± 0.04^{b}
	CD ($P\leq0.05$)	0.257	0.220	0.170

Data followed by the same letter are not significantly different at $P\leq0.05$, where as those followed by different letters are significantly different at $P\leq0.05$.

Table 2 *In-vitro* antifungal studies of fungi present in drinking water PVC pipelines using Citrate coated silver nanoparticles as inhibitors

S. no	Fungi	Citrate coated silver nanoparticles nanoparticles Zone of inhibition (mm)		
		170 ppm	100 ppm	30 ppm
1.	*Meyerozyma caribbica*	1.1 ± 0.15^{de}	0.6 ± 0.06^{bc}	0.2 ± 0.02^{bc}
2	*Aspergillus parvisclerotigenus*	1.2 ± 0.08^{cd}	0.8 ± 0.04^{a}	0.3 ± 0.03^{ab}
3.	*Meyerozyma guilliermondii*	1.4 ± 0.09^{bc}	1.0 ± 0.03^{a}	0.4 ± 0.05^{abc}
4.	*Rhizopus oryzae*	1.0 ± 0.07^{de}	0.5 ± 0.12^{c}	0.1 ± 0.13^{b}
5.	*Uncultured fungus clone*	0.8 ± 0.04^{ef}	0.7 ± 0.08^{ab}	0.3 ± 0.13^{ab}
6.	*Aspergillus oryzae*	0.9 ± 0.09^{ef}	0.8 ± 0.14^{a}	0.6 ± 0.05^{ab}
7.	*Trichoderma asperellum*	1.8 ± 0.06^{a}	0.7 ± 0.06^{ab}	0.4 ± 0.12^{abc}
8.	*Meyerozyma caribbica*	1.6 ± 0.07^{ab}	1.2 ± 0.17^{a}	0.9 ± 0.15^{a}
	CD ($P\leq0.05$)	0.210	0.195	0.190

Data followed by the same letter are not significantly different at $P\leq0.05$, where as those followed by different letters are significantly different at $P\leq0.05$.

investigations directed to better understanding of interaction between silver nanoparticles and bacterial components should shed light on the mode of action of this nanomaterial as a biocidal material.

4. Conclusions

The citrate coated silver nanoparticles have been proved to be one of the potential sources of

antimicrobial agents which showed significant antimicrobial activity against an array of microbes isolated from the drinking water PVC pipe lines.

• The formed CAgNPs are highly stable and polydispersed with the mean size of 50nm. At higher concentrations (170 ppm), significant antimicrobial activity of CAgNPs has been recorded against fungal sp. and Gram-positive and Gram-negative bacteria.

• The higher anti microbial activity of smaller sized nanoparticles could be due to the large surface area to volume ratio with the enhanced surface activity.

• This could be due to the fact that nanoparticles are more abrasive in nature than bulk $AgNO_3$, thus contributing to the greater mechanical damage to the cell membrane resulting in enhanced fungal effect (Padmavathy and Vijayaraghavan 2008).

• Citrate ions influence the particle growth at early stages by complexing with positively charged Ag^{2+} dimers. However, future studies on the biocidal influence of this nanomaterial on other Gram-positive and Gram-negative bacteria are necessary in order to fully evaluate its possible use as a new antibiofilm material.

• Applications of Ag nanoparticles based on these findings may lead to valuable discoveries in various fields such as medical devices and antimicrobial systems.

Acknowledgements

Authors are thankful to Acharya N G Ranga Agricultural University for providing research facilities at Institute of Frontier Technology, Regional Agricultural Research Station, Tirupati to carry out this part of the research work.

References

Carlson, C., Hussain, S.M., Schrand, A.M., Braydich-Stolle, K.L., Hess, K.L., Jones, R.L. and Schlager, J.J. (2008), "Unique cellular interaction of silver nanoparticles: size-dependent generation of reactive oxygen species", *J. Phys. Chem. B*, **112**(43), 13608-13613.

Cho, K.H., Park, J.E., Osaka, T. and Park, S.G. (2005), "The study of antimicrobial activity and preservative effects of nanosilver ingredient", *Electrochim. Acta*, **51**, 956-963.

Choi, O. and Hu, Z. (2008a), "Size dependent and reactive oxygen species related nanosilver toxicity to nitrifying bacteria", *Sci. Technol.*, **42**, 4583-4590.

Choi, O., Deng, K., Kim, N., Ross, L. and Hu, Z. (2008b), "The inhibitory effects of silver nanoparticles, silver ions, and silver chloride colloids on microbial growth", *Water Res.*, **42**, 3066-3072.

Cynthia, H. and Callaghan, O. (1983), *Assessment of a New Antibiotic*, Eds. Hugo, W.B. and Russel, A.D., *Pharmaceutical Microbiology*, Blackwell Scientific Publications, Oxford.

Davis, R.J. and Liu, Z. (1997), "Titania-silica: a model binary oxide catalyst system", *Chem. Mater.*, **9**, 2311-2324.

Duran, N., Marcato, P.D., Alves, O.L., De Souza, G.I.H. and Esposito, E. (2005), "Mechanistic aspects of biosynthesis of silver nanoparticles by several *Fusarium oxysporum* strains", *J. Nanobiotechnol.*, **3**, 8-14.

Feng, Q.L., Wu, J., Chen, G.Q., Cui, F.Z., Kim, T.M. and Kim, J.O. (2000), "A mechanistic study of the antibacterial effect of silver ions on Escherichia coli and Staphylococcus aureus", *Biomed. Mater.*, **52**, 662-670.

Grier, N. (1983), "Silver and its compounds, disinfection, sterilization and preservation, Philadelphia", *Lea Febiger*, **6**, 375-89.

Hamouda, T. and Baker, J.R. (2000), "Antimicrobial mechanism and action of surfactant lipid preparations

in enteric Gram-negative *Bacilli*", *J. Appl. Microbio*, **89**, 397-402.
Jiang, W., Kim Betty, Y.S., Rutka, J.T. and Chan Warren, C.W. (2008), "Nano particle mediated cellular response is size dependent", *Nat. Nanotechnol*, **3**(3), 145-151.
Kelly, K.L., Coronado, E., Zhao, L.L. and Schatz, G.C. (2003), "The Optical Properties of Metal Nanoparticles the Influence of Size, Shape and Dielectric Environment", *Phys. Chem B*, **107**(3), 668-674.
Kim, T.N., Feng, Q.L., Kim, J.O., Wu, J., Wang, H., Chen, G.C. and Cui, F.Z. (1998), "Antimicrobial effects of metal ions (Ag+, Cu2+, Zn2+) in hydroxyapatite", *J. Mater. Sci. Mater. Med.*, **9**, 129-136.
Kowshik, M., Ashtaputre, S. and Kharrazi, S. (2003), "Extracellular synthesis of silver nanoparticles by a silver-tolerant yeast strain MKY3", *Nanotechnology*, **14**, 95-101.
Kumar Sur, U. (2014), "Biological green synthesis of gold and ailver nanoparticles", *Adv. Nano Res.*, **2**, 3-8
Lehninger, A., Nelson, D. and Cox, M. (1993), *Principles of Biochemistry*, 2nd Edition, Worth, New York.
Liau, S.Y., Read, D.C., Pugh, W.J., Furr, J.R. and Russell, A.D. (1997), "Interaction of silver nitrate with readily identifiable groups: relationship to the antibacterial action of silver ions", *Lett Appl Microbiol.*, **25**, 279-283.
Navarro, E., Piccapietra, F., Wagner, B., Marconi, F., Kaegi, R., Odzak, N., Sigg, L. and Behra, R. (2008), "Toxicity of silver nanoparticles to Chlamydomonas reinhardtii", *Environ. Sci. Technol.*, **42**(23), 8959-8964.
Nurmi, J.T., Tratnyek, P.G., Sarathy, V., Baer, D.R., Amonette, J.E., Pecher, K., Wang, C., Linehan, J.C., Matson, D.W., Penn, R.L. and Driessen, M.D. (2004), "Characterization and properties of metallic iron nanoparticles: spectroscopy, electrochemistry, and kinetics", *Environ. Sci. Technol.*, **39**(5), 1221-1229.
Malarkodi, C., Rajesh Kumar, C., Paul Kumar, S., Vanaja, M., Gnanajobitha, G. and Annadurai, G. (2014), "Biosynthesis and antimicrobial activity of semiconductor nanoparticles against oral pathogens", *Bioinor. Chem. Appl.*, **167**, 347-357.
Padmavathy, N. and Vijayaraghavan, R. (2008), "Enhanced bioactivity of $AgNO_3$ nanoparticles-an antibacterial study", *Sci. Technol. Adv. Mater.*, **9**, 1-7.
Prasad, T.N.V.K.V., Kambala, V.S.R. and Naidu, R. (2011), "A critical review on biogenic silver nanoparticles and their antimicrobial activity", *Curr. Nanosci.*, **7**, 531-544.
Reeves, W. and Andrew, W. (1999), *Clinical Antimicrobial Assay*, Oxford University Press, New York, USA.
Sondi, I. and Salopek-Sondi, B. (2004), "Silver nanoparticles as antimicrobial agent: a case study on *E. coli* as a model for Gram-negative bacteria", *J. Colloid Interface Sci.*, **275**(1), 177-183.
Souza, G.I.H., Marcato, P.D., Duran, N. and Esposito E. (2004), "In IX National Meeting of Environmental Microbiology", Curtiba, PR. (in Brazilian)
Spadaro, J.A., Berger, T.J., Barranco, S.D., Chapin, S.E. and Becker R.O. (1974), "Antibacterial effects of silver electrodes with weak direct current", *Microb. Agent. Chemother*, **6**, 637-643.
Stoimenov, P.K., Klinger, R.L., Marchin, G.L. and Klabunde, K.J. (2002), "Metal oxide nanoparticles as bactericidal agent", *Langmuir*, **18**, 6679-6685.
Uchida, M. (1995), "Antimicrobial zeolite and its application", *Chem Ind.*, **46**, 48-54.
Venkateswara Guptha, K. and Samson Nesaraj, A. (2014), "Solvothermal synthesis and characterization of Silver Nanoparticles," *Adv. Nano Res.*, **2**, 3-8
Wright, G.D. (2005), "Bacterial resistance to antibiotics: enzymatic degradation and modification", *Adv. Drug Deliv. Rev.*, **57**, 1451-1458.
Wright, G.D. (2000), "Resisting resistance: new chemical strategies for battling superbugs", *Chem. Biol.*, **7**, 12-19.
Yakutik, M.I., Shevchenko, G.P. and Rakhmanov, S.K. (2004), "The formation of mono disperse spherical silver particles", *Coll. Surf. A: Physicochem. Eng. Aspec.*, **5**, 175-182.
Yamac, M. and Bilgili, F. (2006), "Antimicrobial activities of fruit bodies and/or mycelial cultures of some mushroom isolates", *Pharm Biol.*, **44**, 660-667.